PNAS RESEARCH ARTICLE | NEUROSCIENCE OPEN ACCESS

Astrocyte-to-microglia communication via Sema4B-Plexin-B2 modulates injury-induced reactivity of microglia

Natania Casden[a], Vitali Belzer[a], Abdellatif El Khayari[b], Rachid El Fatimy[b], and Oded Behar[a,1]

Edited by Christopher Glass, University of California San Diego, La Jolla, CA; received January 15, 2024; accepted April 10, 2024

After central nervous system injury, a rapid cellular and molecular response is induced. This response can be both beneficial and detrimental to neuronal survival in the first few days and increases the risk for neurodegeneration if persistent. Semaphorin4B (Sema4B), a transmembrane protein primarily expressed by cortical astrocytes, has been shown to play a role in neuronal cell death following injury. Our study shows that after cortical stab wound injury, cytokine expression is attenuated in *Sema4B*$^{-/-}$ mice, and microglia/macrophage reactivity is altered. In vitro, Sema4B enhances the reactivity of microglia following injury, suggesting astrocytic Sema4B functions as a ligand. Moreover, injury-induced microglia reactivity is attenuated in the presence of *Sema4B*$^{-/-}$ astrocytes compared to *Sema4B*$^{+/-}$ astrocytes. In vitro experiments indicate that Plexin-B2 is the Sema4B receptor on microglia. Consistent with this, in microglia/macrophage-specific *Plexin-B2*$^{-/-}$ mice, similar to *Sema4B*$^{-/-}$ mice, microglial/macrophage reactivity and neuronal cell death are attenuated after cortical injury. Finally, in *Sema4B*|*Plexin-B2* double heterozygous mice, microglial/macrophage reactivity is also reduced after injury, supporting the idea that both Sema4B and Plexin-B2 are part of the same signaling pathway. Taken together, we propose a model in which following injury, astrocytic Sema4B enhances the response of microglia/macrophages via Plexin-B2, leading to increased reactivity.

astrocyte | microglia | inflammation | Sema4B | Plexin-B2

Significance

In this study, we show that in the brain cortex, Sema4B, a protein mainly expressed by astrocytes, plays a crucial role in enhancing the reactivity of microglia/macrophages via Plexin-B2. These findings reveal a unique molecular signaling pathway instigated by astrocytes toward microglia/macrophages in the context of central nervous system (CNS) injury, shedding light on the complex interplay between astrocytes and microglia/macrophages. Taken together, our findings suggest that targeting the Sema4B/Plexin-B2 pathway could be a promising therapeutic approach for reducing microglia/macrophage reactivity and improving the adaptive response in the context of CNS injury.

Brain injury results in the release of damage-associated molecular patterns (DAMPs) which induce inflammation (1). Although this response is critical to limit damage, it has also been reported to exacerbate damage, including neuronal loss (2). Following this acute phase, inflammation may persist and increase the probability of developing a neurodegenerative disease (3). Two of the major types of cells immediately affected by DAMPs are microglia and astrocytes.

Microglia rapidly respond to injury with dramatic morphological transformation (1). In their reactive state, microglia can serve diverse beneficial functions essential to neuronal survival (4). However, reactive microglia can also induce detrimental neurotoxic effects (5). Following injury, immune cells including macrophages infiltrate the brain tissue near the injury site. Since many of the markers are shared with microglia and macrophages, it may be challenging to differentiate between the two.

Astrocytes also respond to injury through a process called reactive astrogliosis which is characterized by changes in gene expression, morphology, and proliferation (6, 7). This response has both beneficial and detrimental effects on inflammation and neuronal survival, as can be inferred by different genetic manipulations in astrocytes (6, 8). It thus appears that astrocyte and microglial reactivity after injury can induce opposing signaling pathways that together determine the degree of inflammation and neuronal cell death. Therefore, finding new molecular modulators of the brain's response to injury may have the potential to affect inflammation and neuronal cell death. One such possible candidate is Sema4B.

Sema4B is a member of the type 4 semaphorins, an evolutionarily conserved family that commonly acts as ligands that bind directly to plexins (9). We have previously shown that Sema4B is expressed by cortical astrocytes and in its absence, the astrocyte reactivity profile is altered, and proliferation is reduced following cortical injury (10). We also showed that neuronal cell death 24 h and 72 h after a stab wound injury is reduced in these *Sema4B*$^{-/-}$ mice (11). These results imply that Sema4B affects the central nervous system's response to injury. However, the mechanism by which Sema4B affects this response is not yet clear.

Results

Expression of Sema4B in the Mouse Brain. To map the cells expressing *Sema4B* in the cortex, we used double in situ hybridization with probes for *Sema4B*, along with either *Sox9* (astrocyte marker) or *CX3CR1* (microglia/macrophage marker). Most cells in the cortex expressing *Sema4B* are also *Sox9* positive while only a small minority of *Sema4B* positive

Author affiliations: [a]Department of Developmental Biology and Cancer Research, The Institute for Medical Research-Israel-Canada, Faculty of Medicine, The Hebrew University, Jerusalem 91120, Israel; and [b]Institute of Biological Sciences (ISSB-P), UM6P Faculty of Medical Sciences, Mohammed VI Polytechnic University, Ben-Guerir 43150, Morocco

Author contributions: N.C. conducted research and analyzed data for Figs. 1, 3-6, S1, and S3-S11; V.B. conducted research and analyzed data for Fig. 2A-C and E; A.E.K. conducted research and analyzed data for Fig. 2D, F, G, and S2; R.E.F. analyzed data in Fig. 2; N.C., A.E.K., and R.E.F. edited the manuscript; O.B. designed research; O.B. supervised data analysis; and O.B. wrote the paper.

The authors declare no competing interest.

This article is a PNAS Direct Submission.

[1]To whom correspondence may be addressed. Email: oded.behar@mail.huji.ac.il.

This article contains supporting information online at https://www.pnas.org/lookup/suppl/doi:10.1073/pnas.2400648121/-/DCSupplemental.

Published May 23, 2024.

cells are also positive for *Cx3Cr1* (Fig. 1 *A*–*C*). Additionally, most astrocytes express *Sema4B* (85.69% ± 5.59) while only a minority of the microglia/macrophages express *Sema4B* (10.66% ± 2.1).

The Inflammatory Response Is Altered in Sema4B Knockout Mice. To test the inflammatory response in *Sema4B* knockout ($Sema4B^{-/-}$) and heterozygous ($Sema4B^{+/-}$) mice following injury, the mRNA of various cytokines was examined (Fig. 2*A* and *SI Appendix*, Fig. S1*A*). In $Sema4B^{-/-}$ mice, some proinflammatory factors (*CCL2*, *CCL3*, *CCL5*, and *IL-6*) were significantly lower 12 h after injury. We also compared $Sema4B^{+/+}$ and $Sema4B^{+/-}$ but did not detect significant differences between the two and thus we continued to use $Sema4B^{+/-}$ as the control during the study (*SI Appendix*, Fig. S1*B*). At 18 h however, *CCL2*, and *IL-6* were more highly expressed in the $Sema4B^{-/-}$ mice, suggesting the differences for some of these inflammatory genes may represent a shift in the kinetics. At the protein level, we tested IL-12, IL-18, IL-10, and IL-1β 24 h after injury using ELISA (Fig. 2*B* and *SI Appendix*, Fig. S1*C*). Both IL-12 and IL-1β were lower in $Sema4B^{-/-}$ mice 24 h after injury, although only IL-12 reached statistical significance.

To test the changes in gene expression more systematically, we isolated astrocytes and immune cells from the injury site 12 h after injury and performed RNAseq. When comparing the astrocytes from $Sema4b^{+/-}$ and $Sema4B^{-/-}$ mice, we detected only one differentially expressed gene (*GM10800*, Fig. 2*C*). In contrast, 102 upregulated and nine downregulated genes were identified in the immune fraction of $Sema4B^{-/-}$ mice (Fig. 2 *C* and *D*). We validated these results by repeating the immunopanning separation and testing three genes from the list in the immune cell fraction (Fig. 2*E*). Since inflammation in $Sema4B^{-/-}$ mice is altered, we focused on genes related to the immune response. To find these genes, we used the gene set enrichment analysis (GSEA) software using the Molecular Signatures Database (MSigDB) (12, 13). We tested *ATF3*, a negative regulator of the inflammatory response, and as such might be expected to dampen the inflammatory response of microglia/macrophages (14). We also examined *Txnip*, which is known to mediate glucocorticoid-activated NLRP3 inflammatory signaling in microglia (15). Finally, we assessed *CD200*, since it is expressed in microglia under certain conditions (16) and plays a significant role in maintaining microglia in a quiescent state and functions as an anti-inflammatory signal (17). To get a sense of the changes in gene expression in the immune fraction of $Sema4B^{-/-}$ mice, we used the list of the genes preranked according to their log2Fold change. We then used the WikiPathway database (*Mus musculus*) to map the preranked genes to their respective enrichment pathways and gene sets (Fig. 2*F*). The GSEA enrichment plots of dysregulated pathways (Fig. 2*G* and *SI Appendix*, Fig. S2*A*) and heatmap displaying the normalized expression of leading genes in three of the main dysregulated pathways related to microglial functions are presented, including toll-like receptors mediating microglial phagocytosis and IFNg signaling (*SI Appendix*, Fig. S2*B*).

Altered Response of Microglia/Macrophages in the Absence of *Sema4B*. To test microglia/macrophage reactivity, we used a morphology analysis using Iba1, a microglia/macrophage-specific marker, to visualize the cells. The cell morphology changes from a ramified state to a more amoeboid shape as it becomes more reactive (Fig. 3*A*). The cells were stained for Iba1 24 h after injury, and the morphological analysis was performed (Fig. 3 *B*–*F*). The results are consistent with enhanced microglia/macrophage reactivity in $Sema4B^{+/-}$ mice as compared to $Sema4B^{-/-}$ mice, though the number of Iba1-positive cells is the same (Fig. 3*G*). Importantly, there were no morphological differences between genotypes in the contralateral side, indicating that there is no difference in their basal state. To get a sense of the significance of the morphological analysis between the two genotypes, we challenged wild-type mice with LPS and tested their morphology after 24 h. The differences with and without LPS are small and reach statistical significance only in one parameter (*SI Appendix*, Fig. S3). We therefore conclude that the differences detected between *Sema4B* knockouts and heterozygous mice after injury are biologically meaningful.

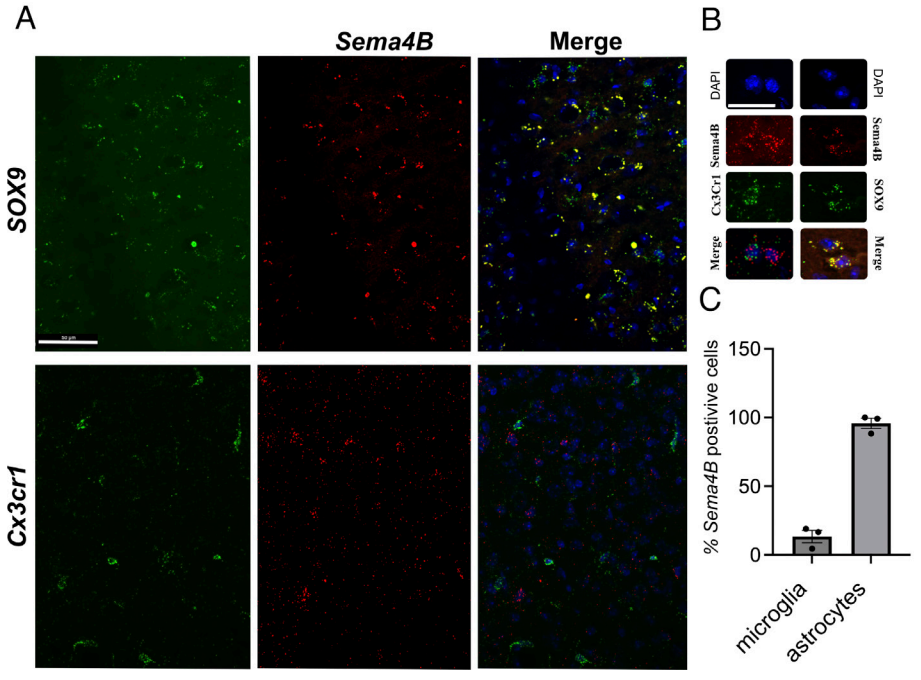

Fig. 1. In situ RNA expression of Sema4B in the adult cortex. (*A*) Representative cortical images stained with probes for Sema4B and Sox9 (*Upper*) or Sema4B and Cx3cr1 (*Lower*). (Scale bar: 50 μm.) (*B*) Example of microglia/macrophages and astrocytes expressing Sema4B. (Scale bar: 25 μm.) (*C*) The percentage of cells positive for Sema4B/Cx3cr1 and Sema4B/Sox9 is presented (n = 3 mice, each data point is an average of three sections per mouse).

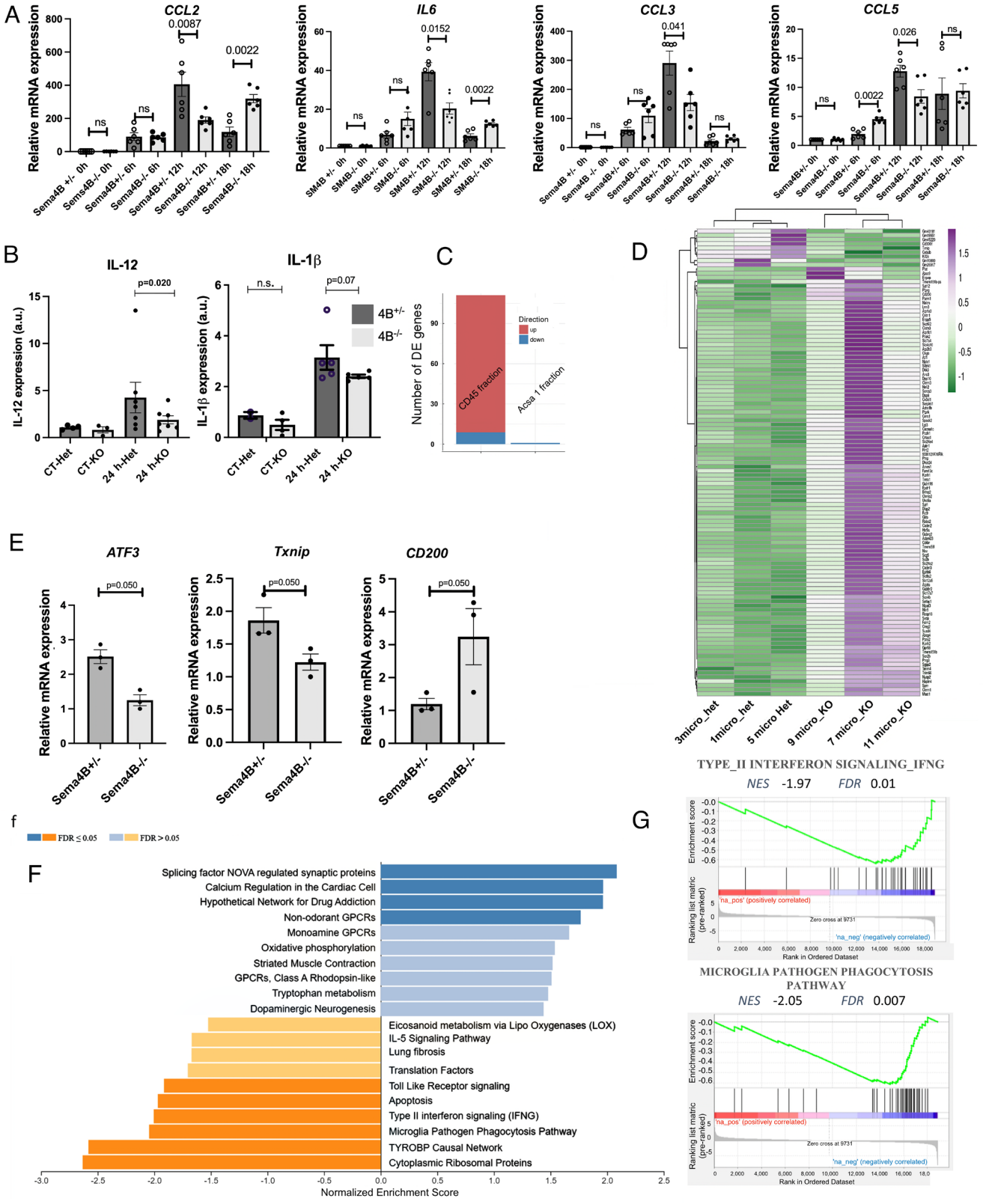

Fig. 2. The inflammatory response following cortical stab wound injury is attenuated in the absence of Sema4B. (*A*) qPCR analysis of the cortical tissue near the site of injury isolated from Sema4B$^{+/-}$ and Sema4B$^{-/-}$ mice at the indicated time points after stab injury (n = 6 mice; Mann–Whitney two-tailed test). (*B*) Levels of inflammatory cytokines 24 h after cortical injury at the site of injury were evaluated using ELISA (n = 5 to 7 mice; Fisher's combined probability test). (*C*) RNAseq analysis of the immune and astrocytic cell fractions isolated by panning 12 h after cortical injury. Plots summarizing the overall number of differentially expressed genes (DEGs). Genes with *P*adj < 0.05 and |log2FoldChange (FC)| > 1 were identified as significant DEGs. (n = 3 repeats, with five mice per genotype within each repeat). (*D*) Heatmap displaying normalized expression levels of significantly dysregulated genes (I LogFC I > 1; *P*-adj value < 0.05) in the immune fraction. (*E*) qPCR analysis of the immune cell fraction isolated by panning (CD45) 12 h after injury (n = 3 groups of five mice each, each data point represents 1 group; Mann–Whitney one-tailed test). (*F*) Gene Set Enrichment Analysis (GSEA) showing significantly dysregulated canonical pathways in the Sema4B$^{-/-}$ immune fraction. GSEA was performed using the Wikipathway database (Mus musculus) with genes preranked according to their log2Fold change. Up-regulated gene-sets are highlighted in blue and down-regulated pathways in orange. (*G*) Enrichment plots for two of the most down-regulated pathways in knockout microglia/macrophages: microglia pathogen phagocytosis pathway (*Left*) and type-II interferon signaling (*Right*).

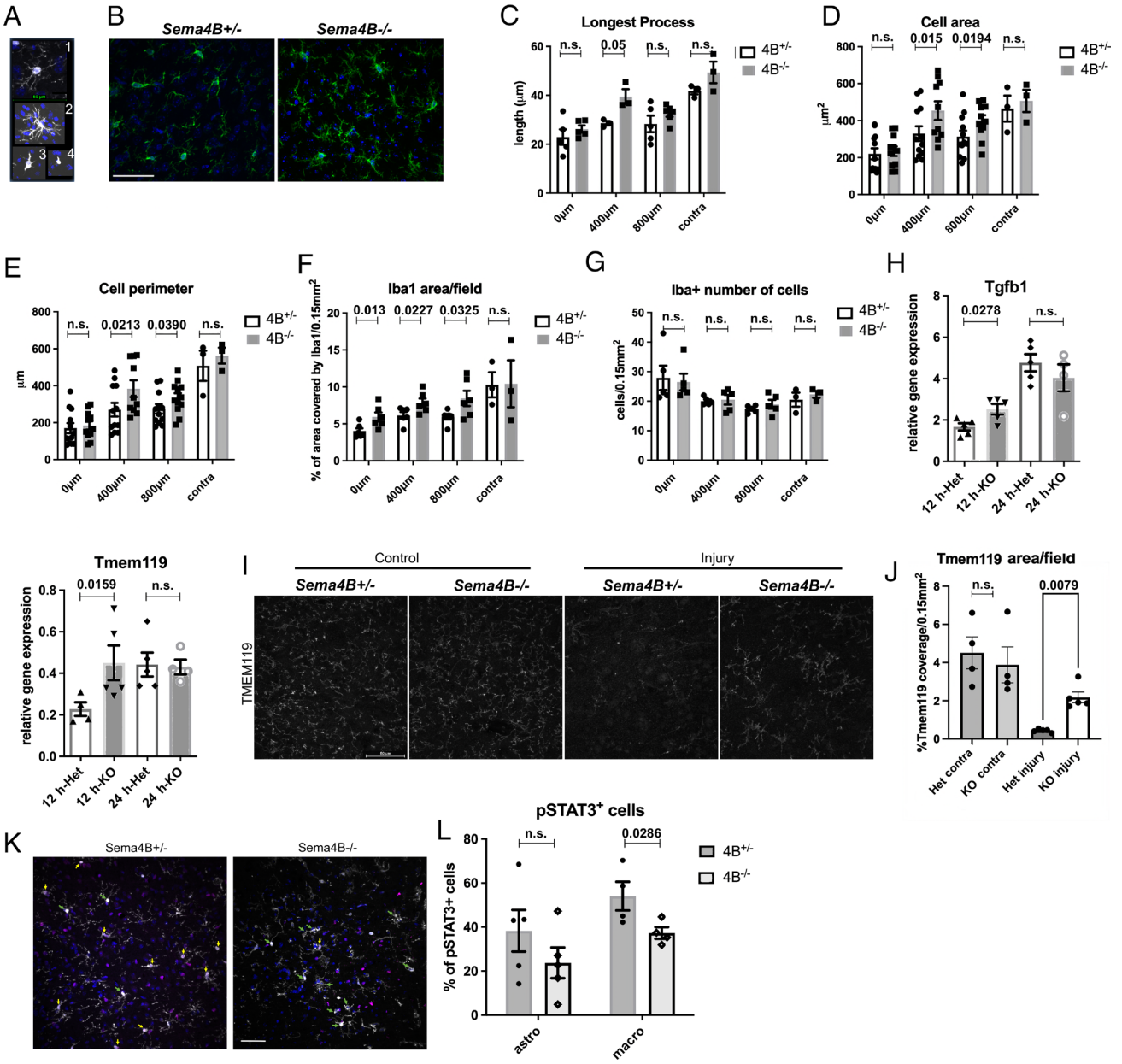

Fig. 3. The reactivity of microglia/macrophages in Sema4B mutant mice is attenuated. (*A*) Examples of microglia/macrophage cells stained with Iba1 (gray) and DAPI (blue) from most ramified (1) to the most ameboid cells (4). (Scale bar: 50 µm.) (*B*) Sections from Sema4B$^{+/-}$ and Sema4B$^{-/-}$ mice 24 h after injury, approximately 800 µm from the injury site, with Iba1 staining (gray) and DAPI (blue). (Scale bar: 50 µm.) (*C*–*E*) Average morphological measurements of the three most amoeboid cells per image in Iba1 stained sections from Sema4B$^{+/-}$ and Sema4B$^{-/-}$ mice at different distances from the injury site and in the contralateral hemisphere. (*C*) longest process (n = 3 to 5 mice, each data point represents one mouse, three sections/mouse), (*D* and *E*) cell area and cell perimeter (n = 10 to 12 sections, each data point represents one section, four mice, three sections/mouse) (Mann–Whitney one-tailed test). (*F*) Mean percent of area coverage of Iba1 staining per field (n = 6 mice, each data point represents one mouse, three sections/mouse; 0.15 mm^2/section; Mann–Whitney one-tailed test). (*G*) Quantification of the average number of Iba1 positive cells per field (n = 5 mice, each data point represents one mouse, three sections/mouse; Mann–Whitney one-tailed test). (*H*) qPCR analysis of homeostatic genes from cortical tissue near the site of injury isolated from Sema4B$^{+/-}$ and Sema4B$^{-/-}$ mice at the indicated time points after stab injury (n = 4 to 6 mice; Mann–Whitney one-tailed test). (*I*) Representative sections of Tmem119 staining from both Sema4B$^{+/-}$ and Sema4B$^{-/-}$ mice 24 h postinjury from the contralateral hemisphere and approximately 200 µm away from the injury site, with Tmem119 staining. (Scale bar: 50 µm.) (*J*) Mean percent of area coverage of Tmem119 staining per field approximately 200 µm from injury site (n = 5 mice, each data point represents one mouse, three sections/mouse, 0.15 mm^2/section, Mann–Whitney one-tailed test). (*K*) Representative images of Iba1 (gray) and pSTAT3 (magenta) 24 h after cortical injury. Green arrows mark pSTAT3 negative/Iba1 positive, and yellow arrows mark pSTAT3 positive/Iba1 positive cells. (Scale bar: 50 µm.) (*L*) Quantification of Iba1/pSTAT3 and S100b/pSTAT3 cells in Sema4B$^{+/-}$ and Sema4B$^{-/-}$ 24 h after injury (n = 4 to 5 mice, each data point represents one mouse, three sections per mouse; Mann–Whitney one-tailed test).

One characteristic of microglial reactivity is the repression of the homeostatic state (18). To evaluate this, we tested several homeostatic genes, including *Hexb*, *Tgfb1*, *p2yr12*, *p2yr13*, *C1qc*, and *Tmem119* at 6 h, 12 h, and 24 h after injury in wild-type male mice (*SI Appendix*, Fig. S4). Overall, all homeostatic genes were down-regulated after injury although with different kinetics. We then compared the expression of these homeostatic genes between *Sema4B*$^{+/-}$ and *Sema4B*$^{-/-}$ mice 12 and 24 h after injury. Both *TGFβ1* and *Tmem119* were more highly expressed 12 h after injury in *Sema4B*$^{-/-}$ mice (Fig. 3*H*) while no significant difference was detected in the case of the other homeostatic genes tested (*SI Appendix*, Fig. S5). Additionally, we tested the levels of TMEM119 24 h after injury using immunofluorescence. Tmem119 in the contralateral side was similar between the two

genotypes. However, near the injury in *Sema4B*$^{-/-}$ mice, the Tmem119 expression area/field is larger than in *Sema4B*$^{+/-}$ mice (Fig. 3*I*). These results are consistent with a more homeostatic state of microglia in *Sema4B*$^{-/-}$ mice.

An additional aspect of immune activation after injury manifests in the migration of immune cells toward the site of injury (19). To further study the impact of *Sema4B*, we quantified the percent of Tmem119+ (a more microglia-specific marker) cells out of the total Iba1+ cells, the number of F4/80+ (macrophage marker) cells and F4/80+/Tmem119- cells, percent of F4/80+/Tmem119+ cells out of total F4/80+ cells, and number of CD45+ cells (general immune cell marker) and CD45+/Iba+ cells, (*SI Appendix*, Fig. S6). Together, these results indicate that there is no difference in microglial/immune cell migration/accumulation in the injury site in *Sema4B* mutant mice.

IFNg signaling found to be repressed in *Sema4B*$^{-/-}$ mice (Fig. 2 *F* and *G* and *SI Appendix*, Fig. S2*B*) is primarily mediated by STAT signaling. We therefore tested STAT3, a major transcriptional activator involved in the injury response of microglia/macrophages and astrocytes. To test the state of pSTAT3 in the cortex, we costained for pSTAT3 and either Iba1 (Fig. 3*K* and *SI Appendix*, Fig. S7*A*) or S100β (an astrocyte marker) (*SI Appendix*, Fig. S7*B*). Without injury, pSTAT3 is undetectable in the mouse cortex (*SI Appendix*, Fig. S7*C*), however, following injury, it is up-regulated. Interestingly, in *Sema4B*$^{-/-}$ mice, the level of pSTAT3 in the microglia/macrophage population is significantly lower but not in astrocytes (Fig. 3*L*).

Astrocytic Sema4B Modulates the Reactivity of Microglial Cells In Vitro. To assess whether Sema4B can act directly on microglia, we performed a live staining assay on cultured microglia to see whether Sema4B has a binding site on these cells and found that they do indeed (Fig. 4*A*). To test the potential effect of Sema4B on microglia, we used an in vitro system of injury in which conditioned medium was collected from injured mixed glial cells (we named this "injury supernatant" or "iSup") and added to microglial cultures. We tested the expression of different inflammatory cytokines (*CCL2, IL-6, CXCL10, IL-1α, IL-1β,* and *TNFα*) after microglial stimulation with iSup with or without Sema4B for 3 h (Fig. 4*B* and *SI Appendix*, Fig. S8*A*) or 9 h (Fig. 4*C* and *SI Appendix*, Fig. S8*B*). Sema4B by itself was a weak stimulus of microglia in the case of some genes. However, together with iSup, Sema4B activated some inflammatory signals more robustly than just iSup alone. To further test the impact of Sema4B on microglia, we also assessed the percentage of microglia expressing iNOS 24 h after addition of iSup and Sema4B (Fig. 4*D* and *SI Appendix*, Fig. S9). Consistent with the qPCR results, more microglial cells express iNOS following exposure to Sema4B and iSup. Finally, to assess whether astrocytic Sema4B is indeed a modulator of microglial cell activation, we incubated wild-type microglia with *Sema4B*$^{+/-}$ and *Sema4B*$^{-/-}$ astrocytes. The culture was stimulated with iSup and the expression of several inflammatory markers (*Chil3, Psmb8, CD300fl*) that are either expressed predominantly by microglia (*Chil3, CD300fl)* or show differential expression only in cultures of both astrocytes and microglia (*Psmb8*) were tested (Fig. 4*E*). Our results clearly show that astrocytic Sema4B is a modulator of microglia, while the limited expression of Sema4B on microglia is not enough to compensate for it.

Plexin-B2 Is the Receptor of Sema4B in Microglia. The Sema4B receptor in microglia is unknown, although the likely candidate is Plexin-B2 (20). We used qPCR to examine the expression of *Plexin-B2* mRNA and its related family member, *Plexin-B1*, in cortical microglia and the BV2 microglial cell line. In both, *Plexin-B2* is highly expressed while *Plexin-B1* is expressed at much lower levels (Fig. 5*A*). To determine whether Sema4B can activate Plexin-B2, we performed a COS cell collapse assay, an assay commonly used to detect Semaphorin-Plexin signaling (21). Indeed, Sema4B can activate this receptor and cause cell collapse (Fig. 5 *B* and *C*). To investigate the potential role of Plexin-B2 in microglial activation following injury, we crossed *Cx3cr1CreER* mice (22) with *Plexin-B2* floxed mice. Cells targeted with this system include microglia, nonparenchymal CNS macrophages, and selected peripheral macrophages, but notably, exclude shorter-lived monocytes. The protein expression of Plexin-B2 with or without 4-hydroxytamoxifen (4OHT) was tested in microglia in vitro. As expected, *Plexin-B2* is expressed by microglia in culture and this expression is eliminated after the 4OHT treatment (*SI Appendix*, Fig. S10*A*). In response to iSup activation, microglia expressed higher levels of cytokines. This response, however, was no longer enhanced by Sema4B after 4OHT treatment even in control microglia. In fact, it had the opposite effect (*SI Appendix*, Fig. S10*B*). As an alternative, we used the microglial cell line BV2 to test the function of Plexin-B2. Targeting *Plexin-B2* with shRNA reduced *Plexin-B2* expression both at the RNA and protein levels (Fig. 5 *D* and *E*). We tested the expression of a few cytokines in BV2 cells after stimulation with Sema4B (Fig. 5*F*). Sema4B by itself triggered expression (*CXCL10, TNFα, and CCL2*) while cells with a *Plexin-B2* knockdown did not respond to Sema4B. In most cases, the activation of BV2 by iSup was not additive to Sema4B (*SI Appendix*, Fig. S11). In contrast, *IL-1b* expression was not affected by Sema4B alone but was higher with iSup together with Sema4B.

Microglial Plexin-B2 Regulates Microglial Reactivity after Cortical Injury. To ascertain whether Plexin-B2 is important for microglial reactivity, we used the *Cx3cr1creER:PlexinB2*$^{fl/fl}$ mouse model to perform cortical injury. We performed in situ hybridization on *Plexin-B2* and *CX3Cr1* (microglia/macrophage marker) in *PlexinB2*$^{+/fl}$ and *PlexinB2*$^{fl/fl}$ mice and confirmed *Plexin-B2* expression is almost exclusively detected in microglia/macrophage cells and that there is almost no expression in knockout cells (Fig. 6*A*). To test whether the absence of *Plexin-B2* in microglia/macrophages attenuates reactivity after injury, we performed a morphological analysis 24 h after injury (Fig. 6 *B–D*). We also noticed that in *PlexinB2*$^{fl/fl}$ mice, there was an increase in Iba1 expression area/field without a change in Iba1 cell number (Fig. 6 *E* and *F*) suggesting larger microglia/macrophages. Together, these results are consistent with a state of reduced microglial/macrophage reactivity in *Plexin-B2* knockout mice. To test whether the homeostatic state of the microglia is affected by the *Plexin-B2* knockout in microglia, we tested the levels of TMEM119 24 hr after injury using immunofluorescence and found that the Tmem119 expression area/field is larger than in *PlexinB2*$^{+/fl}$ mice (Fig. 6*G*). Together, both the morphological changes and Tmem119 expression level are consistent with reduced reactivity of microglia in *PlexinB2*$^{fl/fl}$. Since in the absence of *Sema4B*, neurons are more protected after injury (11), we evaluated whether this is also the case in *Cx3cr1creER:PlexinB2*$^{fl/fl}$ mice. We stained tissue slices with Fluoro-Jade C (FJC) 24 h after injury (Fig. 6 *H* and *I*), and indeed, as in the case of Sema4B, fewer neurons died in the absence of *Plexin-B2* in microglia/macrophages.

Finally, to assess whether Plexin-B2 in microglia and Sema4B are part of the same genetic cascade, we analyzed the reactivity of microglia/macrophages in double heterozygotes for both microglial *Plexin-B2* and *Sema4B*. We detected some changes in

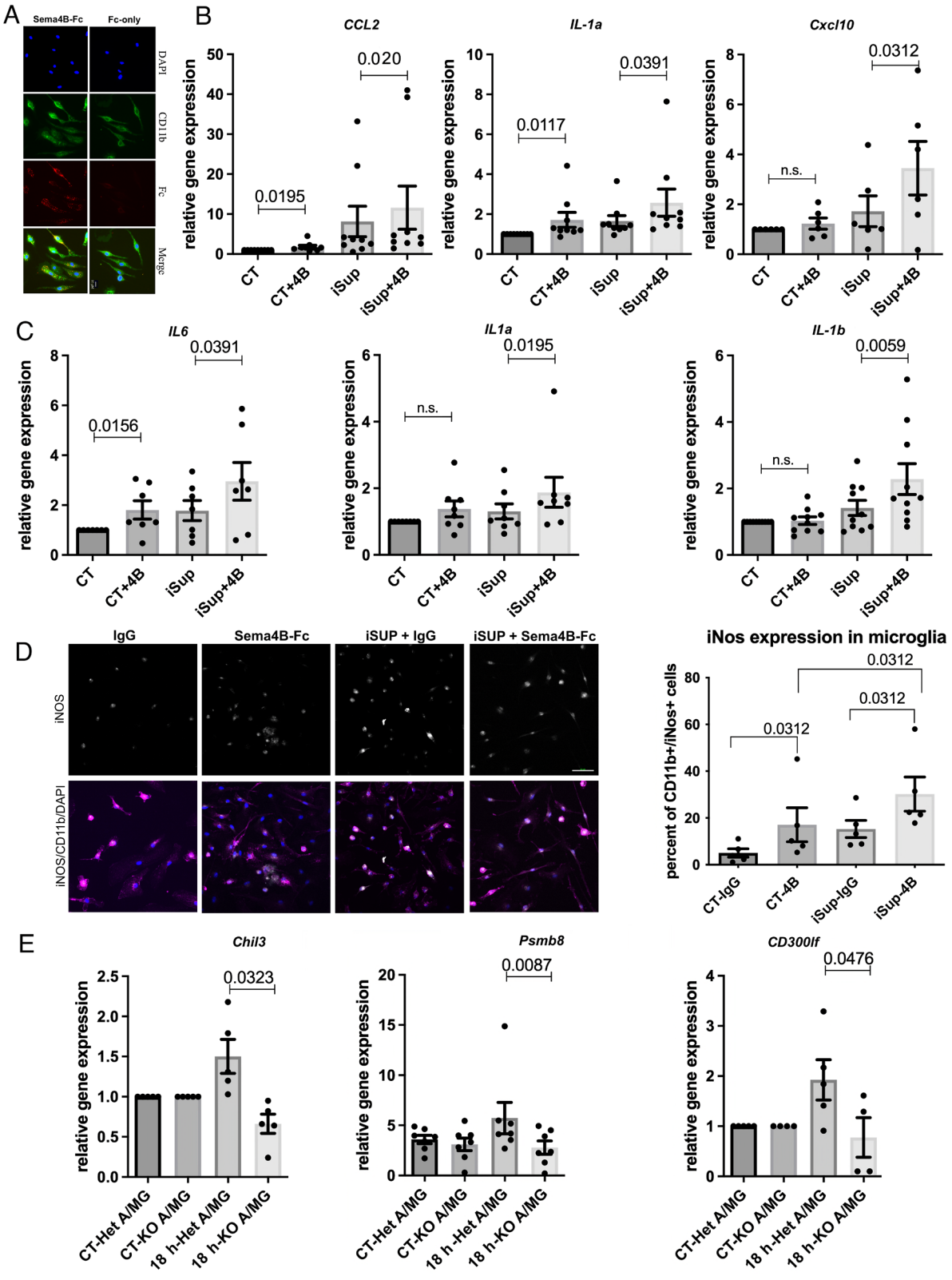

Fig. 4. Sema4B amplifies the reactivity of cultured microglia following injury. (*A*) Live staining of cultured cortical microglia with Sema4B-Fc or Fc-only (red) and CD11b (green). (Scale bar: 10 μm.) (*B* and *C*) qPCR analysis of cultured microglia incubated with HEK293 cells expressing the full-length Sema4B or GFP, and/or iSup for 3 h (*B*) or 9 h (*C*) (n = 6 to 9 independent experiments; Wilcoxon one-tailed test). (*D*) Representative images of iNOS (gray) and CD11b (magenta) staining of cultured microglial cells expressing iNOS 24 h after treatment. (Scale bar: 50 μm.) Quantification of percent of microglial cultured cells expressing iNOS 24 h after treatment with 500 ng of either an IgG control or Sema4B-Fc and/or iSup. Slide fields were chosen at random and quantified (n = 4 independent experiments, each data point represents an average of three fields/experiment; Wilcoxon one-tailed test). (*E*) qPCR analysis of cocultured wild-type microglia (MG) with astrocytes (A) isolated either from Sema4B$^{+/-}$ or Sema4B$^{-/-}$ mice and treated with iSup for 18 h (n = 6 independent experiments; Wilcoxon one-tailed test).

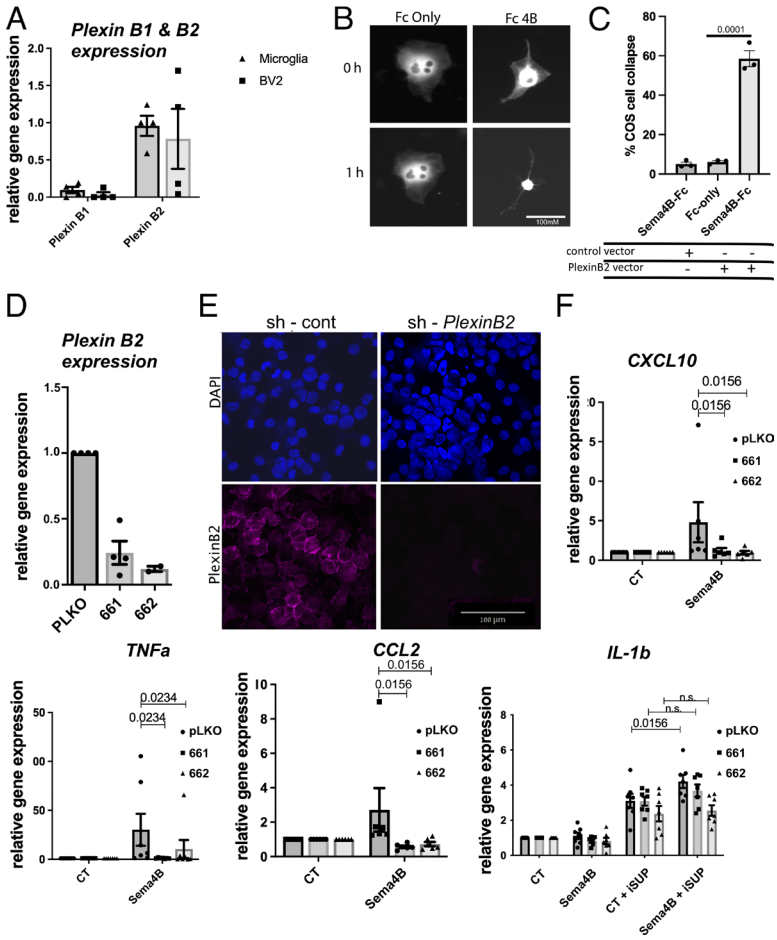

Fig. 5. Plexin-B2 is the likely receptor for Sema4B in microglia. (*A*) qPCR analysis of Plexin-B1 and B2 expression in cultured microglia and BV2 microglial cell line (n = 4). (*B* and *C*) COS cell collapse assay was used to test the potential of Sema4B to function as a ligand for Plexin-B2. (*B*) representative image of a COS cell before and 1 h after treatment with Sema4B-Fc or Fc only. (Scale bar: 100 μm.) (*C*) Quantification of COS cell collapse is shown (n = 3 experiments, each data point represents one experiment, in each experiment at least 100 cells in each condition were evaluated; two-tailed *t* test). (*D*) qPCR analysis of Plexin-B2 expression in BV2 cells treated with two shRNA sequences targeting Plexin-B2 (n = 2 to 4 experiments). (*E*) Representative image of Plexin-B2 immunofluorescence of BV2 cells with scrambled shRNA sequence or shRNA targeting Plexin-B2. (*F*) qPCR analysis of expression of different cytokines (CXCL10, TNFα, CCL2, and IL1β) in BV2 cells transduced with Plexin-B2 shRNA lentiviruses. The BV2 cells were then cocultured with HEK293 cells expressing either full-length Sema4B or GFP, in the presence or absence of iSup for 3 h (n = 6 to 7 independent experiments; Wilcoxon one-tailed test).

microglia/macrophage morphology consistent with a reduction in microglial/macrophage reactivity after injury in these mice (Fig. 6 *J*–*M*), supporting a link between Plexin-B2 on microglia and astrocytic Sema4B in the same genetic signaling cascade.

Discussion

Brain injury triggers a response aimed at restoring homeostasis and limiting damage. A critical part of this response requires coordinated activation of microglia/macrophages and astrocytes. Here, we showed that following cortical injury, Sema4B enhances the reactivity of microglia/macrophages via the Plexin-B2 receptor, and thus, the crosstalk between Sema4B and Plexin-B2 modulates the microglial/macrophage proinflammatory response following injury.

Sema4B Is a Modulator of Inflammatory Response. Semaphorins were originally identified as axon-guidance molecules. Over the years, other functions have been discovered, including in the immune system (23). Many semaphorins with immunological function belong to the type 4 semaphorins and include Sema4D as a prominent example (23). In the CNS, Sema4D was shown to induce microglial cell reactivity and in its absence, cell death is reduced in ischemic stroke (24–26). It seems that Sema4B may play a similar role. We have recently shown that neuronal cell death in cortical injury is reduced in the absence of *Sema4B* (11). We now show here that in the absence of *Sema4B* in mice, reactivity of microglial cells is attenuated. Consistent with this, cultured microglia challenged by injury are more reactive in the presence of Sema4B. Therefore, both Sema4B and Sema4D under conditions of brain injury act as ligands to promote a proinflammatory response.

Plexin-B2 Is a Microglial Receptor for Sema4B. Plexin-B1 and B2 are considered type 4 semaphorin receptors (9). In microglia, both RNA sequencing and single-cell RNA sequencing studies suggest that Plexin-B2 is the primary PlexinB-expressed gene, whereas Plexin-B1 is more highly expressed in astrocytes (27–29) Moreover, recent findings show that Plexin-B2 plays a crucial role as a receptor in microglia/macrophages following spinal cord injury, regulating cell corralling, and that its absence can lead to diffuse tissue damage, inflammatory spillover, and hindered axon regeneration (30).

The Sema4B receptor is still incompletely defined, although Plexin-B2 mutants and ErbB2 phosphorylation assays strongly support Plexin-B2 as the Sema4B receptor in epithelial cells (20).

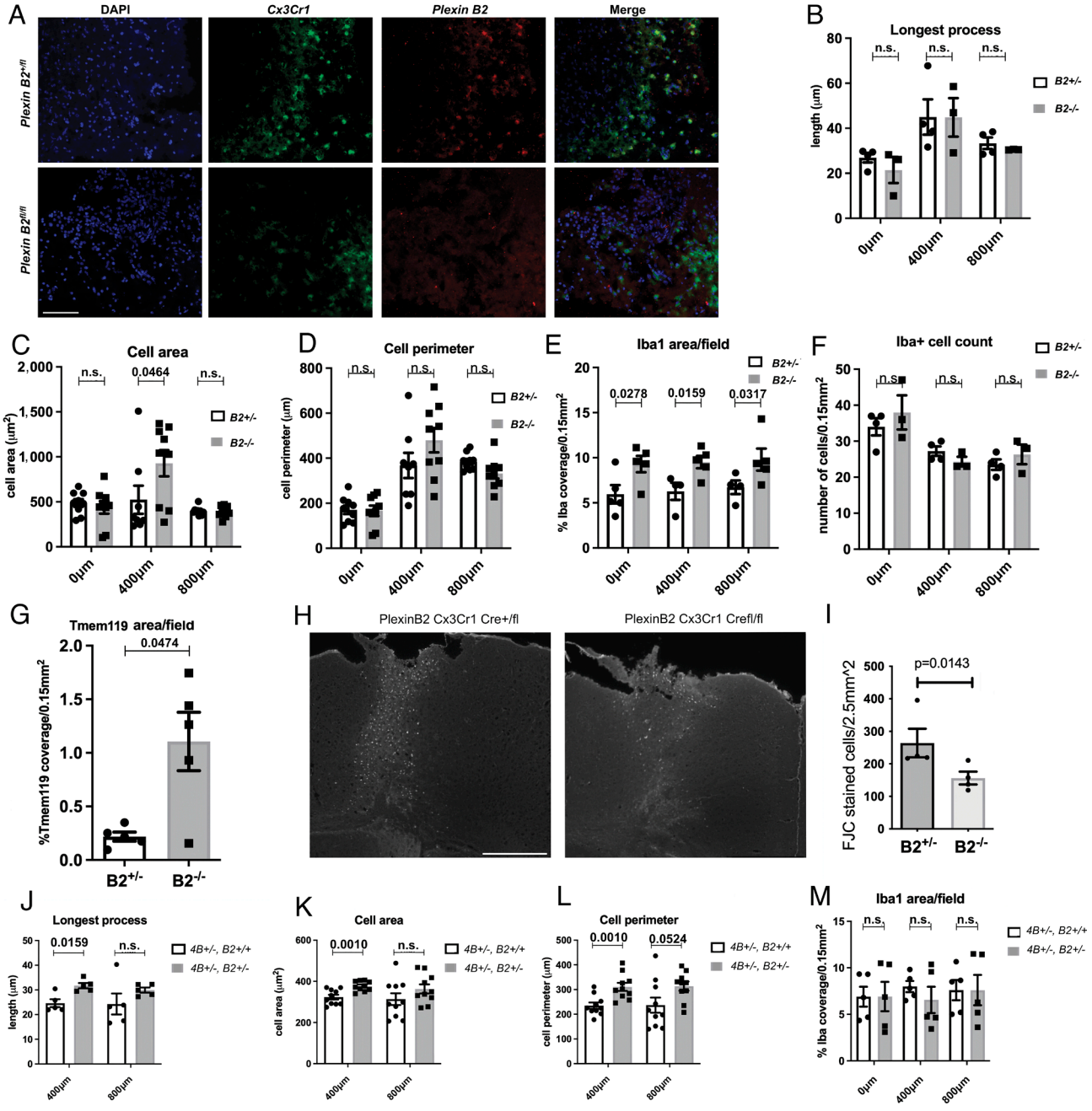

Fig. 6. Microglia/macrophage reactivity is attenuated in Cx3cr1creER:PlexinB2$^{fl/fl}$ mice. (*A*) In situ hybridization of Plexin-B2 and Cx3Cr1 on Cx3cr1creER:PlexinB2$^{+/fl}$ and Cx3cr1creER:PlexinB2$^{fl/fl}$ mice, 3 d after injury. Note that most cells expressing PlexinB2 are Cx3Cr1 positive and that this expression is almost undetected in PlexinB2$^{fl/fl}$ mice. (Scale bar: 50 μm.) (*B–D*) Average morphological measurements of Iba1 images in Cx3cr1creER:PlexinB2$^{fl/fl}$ and Cx3cr1creER:PlexinB2$^{+/fl}$ control mice at different distances from the injury site (*B*: n = 3 to 4 mice, 2 to 3 sections/mouse; (*C* and *D*: n = 8 to 10 sections, 2 to 3 sections/mouse, 3 to 4 mice; Mann–Whitney one-tailed test). (*E*) Mean percent of area coverage of Iba1 staining per field (n = 4 to 5 mice, three sections/mouse; 0.15 mm^2/section, Mann–Whitney one-tailed test). (*F*) Average number of Iba1 positive cells per field (n = 5 mice, three sections/mouse; Mann–Whitney one-tailed test). (*G*) Median percent of area coverage of Tmem119 staining per field approximately 200 μm from injury site (n = 5 mice, three sections/mouse, 0.15 mm^2/section, Mann–Whitney one-tailed test). (*H*) Representative coronal cortical sections in Cx3cr1creER:PlexinB2$^{fl/fl}$ and Cx3cr1creER:PlexinB2$^{+/fl}$ mice 1 d after injury. The panel shows dead neurons labeled with FJC. (Scale bar: 500 μm.) (*I*) Average number of dead neurons (FJC positive) per field 1 d after injury (n = 4 mice, 4 to 6 sections/mouse; Mann–Whitney one-tailed test). (*J–M*) Average morphological measurements of Iba1 images in Sema4$^{+/-}$/Cx3cr1creER:PlexinB2$^{+/+}$ and Sema4$^{+/-}$/PlexinB2$^{+/fl}$ mice measured 400 and 800um from the injury site (*J*: n = 5 mice, two sections/mouse, *K* and *L*: n = 10 sections, two sections/mouse, five mice, *M*: n = 5 mice, three sections/mouse, 0.15 mm^2/section; Mann–Whitney one-tailed test).

Our own experiments show that Sema4B can bind Plexin-B2 and serve as a functional receptor in a COS cell collapse assay. We also find that in a microglial cell line, Sema4B-induced cytokine expression is Plexin-B2 dependent. Moreover, the similar impact of *Sema4B* and *Plexin-B2* knockouts on microglial/macrophage reactivity is consistent with crosstalk between these two receptor–ligand pairs, a conclusion supported by the genetic interaction between these two genes.

Does Sema4B Function As a Ligand or Receptor after Brain Injury? Our earlier study showed that 7 d after injury, astrocyte proliferation is diminished while reactivity is changed, and our in vitro experiments indicate that injury-induced astrocyte proliferation is cell-autonomous and reliant on Sema4B phosphorylation, thus suggesting Sema4B's role as a receptor in astrocytes (10). In contrast, the impact of Sema4B on inflammation in general, and microglia specifically, presented in the current

study shows a ligand function of Sema4B. Interestingly, although both *Plexin-B2* deletion in microglia and *Sema4B* knockout affect microglial/macrophage reactivity, the latter seems to have a more pronounced impact. This may be explained by a dual function of Sema4B both as a ligand and as a receptor, however, future studies will be needed to test this hypothesis.

Microglia–Astrocyte Communication via Plexin-B2 and Sema4B. The findings presented in this study, along with previous research, indicate that in the cortex Sema4B is expressed by astrocytes, with some expression observed in a minority subpopulation of microglia (10, 28, 31). Although we employed a global Sema4B knockout mouse model in this study and cannot definitively rule out the potential contribution of microglial Sema4B, our astrocyte–microglia coculture system clearly illustrates that microglial-Sema4B is unable to compensate for the absence of astrocytic Sema4B. Thus, our results support the crucial role of astrocytic Sema4B in modulating microglial reactivity after injury. Based on these results, we propose a model in which astrocytic Sema4B acts through the Plexin-B2 receptor under injury conditions to enhance DAMP-triggered reactivity of microglia. As a result, inflammation following a cortical stab wound injury is amplified.

In summary, our study provides unique insights into the complex cellular mechanisms involved in the response to brain injury and highlights the potential of Sema4B and Plexin-B2 as a therapeutic target for intervention.

Materials and Methods

Study Design. We conducted a series of studies to investigate the role of Sema4B during cortical injury. To simulate injury, we employed a stab wound in vivo and used conditioned media from injured mixed cortical cultures to emulate injury conditions in vitro. To assess the function of Sema4B, we utilized Sema4B knockout mice, purified astrocytes from these mutations, and recombinant Sema4B. Despite Sema4B being predominantly expressed by astrocytes, RNA sequencing revealed that microglia/macrophages were the cells most significantly impacted in the absence of Sema4B.

This effect on microglia/macrophages was confirmed by evaluating the reactivity state of the cells through both in vivo and in vitro strategies. Ultimately, we established that PlexinB2 serves as the receptor for Sema4B on microglia/macrophages and demonstrated that manipulating this receptor yields similar outcomes as manipulating Sema4B itself.

Antibody and primer information can be found in *SI Appendix, Extended Methods*.

Animals and Surgical Procedure. Animal handling adhered strictly to national and institutional guidelines for animal research and was approved by the Ethics Committee of the Hebrew University.

Sema4B$^{+/-}$ mutant mice were bought from the Mutant Mouse Regional Resource Center (MMRRC) and used as described previously (10). The generation of *PlxnB2* conditional knockout mice was described previously (31). *CX3Cr1CreER* mice from ref. 22 were crossed with floxed *Plexin B2* mice for the KO experiments. C57BL/6 wild-type mice were obtained from ENVIGO. All cortical injury experiments were performed on mice aged 7 to 12 wk. Genotype was determined by PCR analysis of genomic DNA isolated from ear clippings of 3-wk-old mice (additional information can be found in supplementary). In all experiments, both males and females were used in similar numbers, except for *SI Appendix*, Figs. S5 and S6*A* and Fig. 3*H* in which we used males only. Extended information regarding the mice work, tamoxifen treatment, stab wound injury model, and LPS injections are in *SI Appendix, Extended Methods*.

In Situ Hybridization. Specific probes for *SOX9*, *Sema4B*, *Plexin-B2,* and *Cx3Cr1* were purchased from molecular Instruments and were used with their HCR™ RNA-FISH Technology kit according to manufacturer protocol (32).

Cell Culture. Astrocytes and microglia were cultured and purified as described in *SI Appendix, Extended Methods*.

Immunofluorescence, Fluoro-Jade C Staining, RNA Extraction, Protein Harvesting, ELISA, and qPCR. Explanations can be found in *SI Appendix, Extended Methods*.

RNA Seq and Bioinformatics Analysis.

Cell isolation by immunopanning. First, cortical tissue (3 mm × 3 mm) around the stab wound injury from three mice for each genotype was dissected out and the white matter was peeled off. Cell immunopanning was performed essentially as previously described (33). Cortical tissue was dissociated into cells using 200 u/mL papain (cat # LS003126, Worthington) and DNAse followed by trituration. The cells were added to the secondary-only plate, followed by sequential incubation in plates containing antibodies against CD45, Thy1, O4, and finally ACSA-2. RNA was extracted from plates 1 + 2 (immune fraction) and the ACSA-2 plate (astrocytes), using Direct-zol™ RNA Mini-Prep (Zymo Research) kit. All samples had a 260/280 OD of at least 1.93 (and an average of 2), and a RIN value of at least 8.

The antibodies used in the panning experiments are indicated in *SI Appendix, Section*.

Sequencing. RNA-seq libraries were prepared at the Crown Genomics Institute of the Nancy and Stephen Grand Israel National Center for Personalized Medicine, Weizmann Institute of Science. Libraries were prepared using the INCPM-mRNA-seq protocol (a homemade protocol, similar to Truseq by Illumina). Briefly, the polyA fraction (mRNA) was purified from 500 ng of total input RNA followed by fragmentation and the generation of double-stranded cDNA. After Agencourt Ampure XP beads cleanup (Beckman Coulter), end repair, A base addition, adapter ligation, and PCR amplification steps were performed. Libraries were quantified by Qubit (Thermo Fisher Scientific) and TapeStation (Agilent). Sequencing was done on a single lane on a Hiseq2500 V4 50 cycles single read kit (Illumina). The loading concentration was 10 pM, sequencing parametres were rd1-61, i7-11. Sequencing yielded between 18 M and 22 M reads per sample (median of 21,630,000 reads). The average quality was above 35 throughout the sequencing cycles. About 95% of the reads aligned to the mouse genome. These included about 15% of multialigned reads, 15% of uniquely aligned reads outside of known exons, and ~65% of uniquely aligned reads that matched known exons. Thus, a median of 14,270,000 reads per sample was used for further analysis.

Bioinformatics. Poly-A/T stretches, and Illumina adapters were trimmed from the reads using cutadapt (34); resulting reads shorter than 30 bp were discarded. Reads were mapped to the *M. musculus* GRCm38 reference genome using STAR (35), supplied with gene annotations downloaded from Ensembl release 92 (STAR was run with EndToEnd option and outFilterMismatchNoverLmax 0.04). Expression levels for each gene were quantified using htseq-count (36). Differentially expressed genes were identified using DESeq2 (37) with the betaPrior, cooksCutoff and independent filtering parameters set to False. The pipeline was run using snakemake (38). The GEO Submission access number is GSE230069 (39).

Gene set enrichment analysis. The analysis was done with all genes preranked according to their log2Fold change. The Wikipathway database (*Mus musculus*) was employed to map the preranked genes to their respective pathways and gene sets.

IPA pathway analysis. Pathway analysis and enrichment of immune canonical pathways were performed based on the Ingenuity Pathway Analysis (IPA) Interactions Knowledge Base, including direct and indirect relationships between genes and endogenous molecules. Expression data for 1,012 genes were included (genes with P value < 0:01). Signaling pathways with z-score > 1.3 were considered significantly dysregulated. Enrichment of immune pathways, macrophage reactivity, and neuro-inflammation were particularly highlighted.

Microglial Morphological Analysis. The sections were photographed with a spinning disc microscope. The images were processed, analyzed, and measured using ImageJ software. The Z stack was amalgamated using maximum intensity. For the longest cell process, cell area, and cell perimeter the three most ameboid cells per field were analyzed and measured. For the average Iba1 or Tmem119 area/field, the upper threshold of each picture was set to the same value for every set, and % of area above the threshold was measured.

Injury Medium (iSup). iSup was prepared by first washing 10 cm plates of cortical mixed cell cultures with cold PBS, and then scraping the cells from the bottom of the plate in 5 mL of cold cell medium with no serum. Cell chunks

were triturated first with a 1 mL tip and then a 200 μL tip to break them up. The medium was then vortexed and centrifuged at 1,000 g for 10 min at 4 °C. The medium was filtered through a 0.22-μm strainer, and frozen and stored at −80 °C. iSup is added to cell cultures at a dilution of 1:4 of the regular volume of medium, along with 2 μM ATP (Sigma A2383). Cells are washed once with PBS before RNA is extracted.

Sema4B-Fc and Fc Control. The generation of Sema4B and Fc control is described in *SI Appendix, Extended Methods*. The use of this reagent was in Fig. 4 *A* and *D* and Fig. 5 *B* and *C*. In all other experiments (Figs. 4 *B* and *C* and 5*F*), we used HEK293 cells transfected with the entire sequence of Sema4B as described below.

Stimulation of Microglia with Sema4B and iSup. HEK293 cells were transfected with plasmids encoding either the full-length *Sema4b* or *GFP*. Twenty-four hours later, 50,000 microglial cells were cultured with 100,000 HEK293 cells, and the next day, the cells were washed with PBS and incubated with a medium containing no serum (DMEM only) for 24 h. The cells were treated with iSup for the specified amount of time, the RNA was harvested from the cells, and gene expression levels were measured using mouse-specific primers in qPCR.

Plexin-B2 Knockdown in BV2 Cells. For the knockdown experiments, we used MISSION® shRNA lentiviral vectors (pLKO.1) which include a puromycin selection marker: TRCN0000078856 (661) and TRCN0000078857 (662). For control, we used a PLKO vector with a scrambled shRNA sequence. Additional details are in *SI Appendix, Extended Methods*.

COS Cell Collapse Assay. The explanation is found in *SI Appendix, Extended Methods*.

AI software use. ChatGPT was used in some parts of the text editing.

Statistical Analysis. Values presented are mean ± SEM. *P*-value ≤ 0.05 was considered significant.

Statistical analysis was performed using the two-tailed or one-tailed Mann–Whitney *U* test. Where relevant, *P*-values were adjusted for multiple comparisons in accordance with the Bonferroni procedure; overall *P*-values for the different injury experiments were then computed from these adjusted *P*-values using Fisher's chi-square test for combined probabilities. For Elisa, we used Fisher's combined probability test. For microglial reactivity in culture, we used Wilcoxon one-tailed test. Finally, for the COS cell collapse assay, we used a two-tailed *t* test.

Data, Materials, and Software Availability. RNA seq data have been deposited in GEO (GSE230069) (39).

ACKNOWLEDGMENTS. We thank Dr. Rohini Kuner for providing the PlexinB2$^{fl/fl}$ mice. We thank Drs. Thomas Worzfeld and Luca Tamagnone for their critical reading. We also thank Dr. Luca Tamagnone for providing the PlexinB1 and B2 expression vectors. We also thank the Hebrew University, Faculty of Medicine Core Research Facility, and particularly Drs. Zakhariya Manevitch and Yael Feinstein-Rotkopffor for valuable help with microscopy. We are grateful to Dr. Norman Grover (Department of Experimental Medicine, The Hebrew University) for helpful advice regarding the statistical analyses.

1. S. P. Gadani, J. T. Walsh, J. R. Lukens, J. Kipnis, Dealing with danger in the CNS: The response of the immune system to injury. *Neuron* **87**, 47–62 (2015).
2. M. Sochocka, B. S. Diniz, J. Leszek, Inflammatory response in the CNS: Friend or foe? *Mol. Neurobiol.* **54**, 8071–8089 (2017).
3. H. S. Kwon, S.-H. Koh, Neuroinflammation in neurodegenerative disorders: The roles of microglia and astrocytes. *Transl. Neurodegener.* **9**, 1–12 (2020).
4. Z. Chen, B. D. Trapp, Microglia and neuroprotection. *J. Neurochem.* **136** (suppl. 1), 10–17 (2016).
5. G. C. Brown, J. J. Neher, Microglial phagocytosis of live neurons. *Nat. Rev. Neurosci.* **15**, 209–216 (2014).
6. G. Yu, Y. Zhang, B. Ning, Reactive astrocytes in central nervous system injury: Subgroup and potential therapy. *Front. Cell. Neurosci.* **15**, 792764 (2021).
7. C. Escartin *et al.*, Reactive astrocyte nomenclature, definitions, and future directions. *Nat. Neurosci.* **24**, 312–325 (2021).
8. M. V. Sofroniew, Astrocyte reactivity: Subtypes, states, and functions in CNS innate immunity. *Trends Immunol.* **41**, 758–770 (2020).
9. D. Carulli, F. de Winter, J. Verhaagen, Semaphorins in adult nervous system plasticity and disease. *Front. Synaptic Neurosci.* **13**, 672891 (2021).
10. L. Ben-Gigi *et al.*, Astrogliosis induced by brain injury is regulated by sema4b phosphorylation. *eNeuro* **2** (2015), 10.1523/ENEURO.0078-14.2015.
11. S. Sweetat, N. Casden, O. Behar, Improved neuron protection following cortical injury in the absence of Semaphorin4B. *Front. Cell. Neurosci.* **16**, 1076281 (2022).
12. A. Subramanian *et al.*, Gene set enrichment analysis: A knowledge-based approach for interpreting genome-wide expression profiles. *Proc. Natl. Acad. Sci. U.S.A.* **102**, 15545–15550 (2005).
13. V. K. Mootha *et al.*, PGC-1alpha-responsive genes involved in oxidative phosphorylation are coordinately downregulated in human diabetes. *Nat. Genet.* **34**, 267–273 (2003).
14. P. Förstner *et al.*, Neuroinflammation after traumatic brain injury is enhanced in activating transcription factor 3 mutant mice. *J. Neurotrauma* **35**, 2317–2329 (2018).
15. V. Bharti, H. Tan, H. Zhou, J.-F. Wang, Txnip mediates glucocorticoid-activated NLRP3 inflammatory signaling in mouse microglia. *Neurochem. Int.* **131**, 104564 (2019).
16. M.-H. Yi *et al.*, Expression of CD200 in alternative activation of microglia following an excitotoxic lesion in the mouse hippocampus. *Brain Res.* **1481**, 90–96 (2012).
17. X. Zhao, J. Li, H. Sun, CD200-CD200R interaction: An important regulator after stroke. *Front. Neurosci.* **13**, 840 (2019).
18. R. C. Paolicelli *et al.*, Microglia states and nomenclature: A field at its crossroads. *Neuron* **110**, 3458–3483 (2022).
19. M. V. Russo, D. B. McGavern, Immune surveillance of the CNS following infection and injury. *Trends Immunol.* **36**, 637–650 (2015).
20. J. Xia *et al.*, Semaphorin-plexin signaling controls mitotic spindle orientation during epithelial morphogenesis and repair. *Dev. Cell* **33**, 299–313 (2015).
21. T. Takahashi *et al.*, Plexin-neuropilin-1 complexes form functional semaphorin-3A receptors. *Cell* **99**, 59–69 (1999).
22. S. Yona *et al.*, Fate mapping reveals origins and dynamics of monocytes and tissue macrophages under homeostasis. *Immunity* **38**, 79–91 (2013).
23. S. P. Chapoval, Neuroimmune semaphorins as costimulatory molecules and beyond. *Mol. Med.* **24**, 13 (2018).
24. T. Okuno *et al.*, Roles of Sema4D-plexin-B1 interactions in the central nervous system for pathogenesis of experimental autoimmune encephalomyelitis. *J. Immunol.* **184**, 1499–1506 (2010).
25. E. S. Smith *et al.*, SEMA4D compromises blood-brain barrier, activates microglia, and inhibits remyelination in neurodegenerative disease. *Neurobiol. Dis.* **73**, 254–268 (2015).
26. T. Sawano *et al.*, Effect of Sema4D on microglial function in middle cerebral artery occlusion mice. *Glia* **63**, 2249–2259 (2015).
27. Y. Zhang *et al.*, An RNA-sequencing transcriptome and splicing database of glia, neurons, and vascular cells of the cerebral cortex. *J. Neurosci.* **34**, 11929–11947 (2014).
28. T. R. Hammond *et al.*, Single-cell RNA sequencing of microglia throughout the mouse lifespan and in the injured brain reveals complex cell-state changes. *Immunity* **50**, 253–271.e6 (2019).
29. M. L. Bennett *et al.*, New tools for studying microglia in the mouse and human CNS. *Proc. Natl. Acad. Sci. U.S.A.* **113**, E1738–46 (2016).
30. X. Zhou *et al.*, Microglia and macrophages promote corralling, wound compaction and recovery after spinal cord injury via Plexin-B2. *Nat. Neurosci.* **23**, 337–350 (2020).
31. S. Deng *et al.*, Plexin-B2, but not Plexin-B1, critically modulates neuronal migration and patterning of the developing nervous system in vivo. *J. Neurosci.* **27**, 6333–6347 (2007).
32. H. M. T. Choi *et al.*, Third-generation in situ hybridization chain reaction: Multiplexed, quantitative, sensitive, versatile, robust. *Development* **145**, dev165753 (2018).
33. L. C. Foo, Purification of rat and mouse astrocytes by immunopanning. *Cold Spring Harb. Protoc.* **2013**, 421–432 (2013).
34. M. Martin, Cutadapt removes adapter sequences from high-throughput sequencing reads. *EMBnet J.* **17**, 10 (2011).
35. A. Dobin *et al.*, STAR: Ultrafast universal RNA-seq aligner. *Bioinformatics* **29**, 15–21 (2013).
36. S. Anders, P. T. Pyl, W. Huber, HTSeq–a Python framework to work with high-throughput sequencing data. *Bioinformatics* **31**, 166–169 (2015).
37. M. I. Love, W. Huber, S. Anders, Moderated estimation of fold change and dispersion for RNA-seq data with DESeq2. *Genome Biol.* **15**, 550 (2014).
38. J. Köster, S. Rahmann, Snakemake–a scalable bioinformatics workflow engine. *Bioinformatics* **28**, 2520–2522 (2012).
39. N. Casden, V. Belzer, O. Behar, "Analysis of the immune and astrocytic cell fraction 12h after cortical injury in Sema4B knockout mice." GEO [Dataset]. https://www.ncbi.nlm.nih.gov/geo/query/acc.cgi?acc=GSE230069. Deposited 19 April 2023.